Finite Element Simulations for Torsional Performance of Corrugated Steel Web trough girders

Jinlong Liu[1,a], Minghui Zhang[2,b], Jue Lv[3,*], Xin Zhao[3], Yu Zhou[3]

[1]Yunnan Design Institute Group Geotechnical Engineering Institute Co., Ltd., Kunming, Yunnan, 650228, China
[2]School of China University of Mining and Technology, Xuzhou, Jiangsu, 221116, China
[3]Yunnan Design Institute Group Co., Ltd, Kunming, Yunnan, 650228, China

[a]ljlong817@163.com, [b]zmharc2023@163.com, *154404559@qq.com

Abstract. Owing to the advantages of lightweight, high-efficiency pre-stress, crack-resisting, corrugated steel web trough girders (CSWTGs) gain wide applications in rail transit viaduct structures. Viewing the inevitable torque caused by vehicle sway, wind loads, and curved alignments, and the limited research related to the torsional performance of CSWTGs, finite element simulations were constructed and calculated to explore the impact of corrugated steel web thickness, boundary conditions, height-to-span ratio, and aspect ratios on the torsional performance of CSWTGs. Results indicate ultimate torsional capacity of CSWTGs increase with the enhancement of corrugated steel web thickness for typical flexural failure happened when the web thickness higher than 4mm. However, a premature buckling failure happened on the CSWTGs with web thickness of corrugated steel lower than 2mm leading to a huge decline of torsional capacity. Additionally, fixed boundary conditions, higher height-to-span ratio and lower aspect ratios can significantly enhance both the ultimate torsional capacity and torsional stiffness of CSWTGs.

Keywords: Channel beams, Corrugated steel webs, Torsional capacity, Finite element simulation, Parametric analysis.

1 Introduction

Since the active service of the double-track trough girder in Huairou in 1981, trough girders have been extensively utilized in the construction of rail transit systems across China. In recent years, these girders have undergone continuous development to address challenges such as low prestress efficiency and the propensity for web cracking. The introduction of the CSWTGs, comprising a reinforced concrete base, corrugated steel web, and flange plate, marks a significant advancement. Due to factors such as vehicle sway, wind loads, and curved alignments, CSWTGs are subjected to torsional effects that pose a risk of failure. Current research has predominantly concentrated on the construction techniques, bending resistance, and shear performance of these structures, with limited attention given to their torsional performance.

H. Bilgin et al. (eds.), *Proceedings of the 2024 6th International Conference on Civil Engineering, Environment Resources and Energy Materials (CCESEM 2024)*, Advances in Engineering Research 253,
https://doi.org/10.2991/978-94-6463-606-2_13

Research on the torsional performance of channel-shaped beams remains relatively limited. Chen et al.[1-3] conducted torsional capacity tests on four single-channel thin-walled reinforced concrete (RC) beams, revealing that under pure torsion, these members exhibited bending failure governed by warping moments. They subsequently proposed a method for calculating nonlinear torsional characteristics. Xu et al.[4, 5] explored the mechanical behaviour of large-scale reinforced concrete U-shaped thin-walled beams under the combined effects of bending, shear, and torsion through experimental studies. Their findings highlighted significant variations in crack patterns and strain distributions under these combined effects, with the beams ultimately demonstrating ductile bending failure. Huang et al.[6]were pioneers in proposing CSWTGs, introducing a calculation method for the structure's ultimate bending strength and advancing research on construction technology and equipment. Chen et al.[7] conducted torsional capacity tests of a CSWTG, considering the effects of steel plate shear deformation and the accordion effect on the longitudinal and torsional stiffness of the beam.

This study utilizes numerical models based on existing experiments to explore the effects of parameters such as corrugated steel thickness, boundary conditions, height-to-span ratio, and height-to-width ratio on the ultimate torsional capacity and stiffness of CSWTGs, providing technical references for their wider application.

2 Finite Element Modeling

2.1 Research Subject

This study focuses on the CSWTG loaded by Tian [8]. A corresponding numerical model is developed using the ABAQUS platform. The cross-sectional dimensions and construction of the channel beam are illustrated in Figure 1. The beam is 6000mm in length, 510mm in height, and 1200mm in width. Two trapezoidal corrugated steel I-beam were utilized as the webs, bonded to both the flange concrete and the bottom concrete slab through shear studs. Detailed parameters of this channel beam can be found in reference[8].

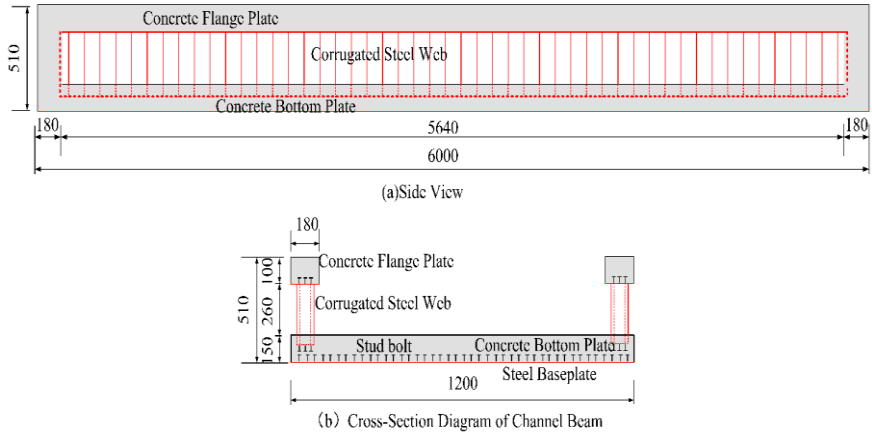

Fig. 1. Cross-Section Dimensions and Construction Diagram of CSWTG

2.2 Material Constitutive Models

In the model, the concrete is described using a plastic damage constitutive definition, as specified in Eq.(1). The parameters for this model include a dilation angle(ψ°) of 36°, an eccentricity value(e) of 0.1, a biaxial compressive strength to uniaxial compressive strength ratio($\sigma_{t0} / \sigma_{c0}$) of 1.16, a stress invariant ratio(K_C) of 0.67, and a viscosity coefficient(υ)of 0.05.

$$\begin{cases} \sigma_t = (1-d_t)E_0(\varepsilon_t - \varepsilon_t^{pl}) \\ \sigma_c = (1-d_c)E_0(\varepsilon_c - \varepsilon_c^{pl}) \end{cases} \tag{1}$$

Where ε_t^{pl} represents the true tensile strain, ε_c^{pl} denotes the true compressive strain, d_c and d_t are the tensile and compressive damage parameters, respectively, and E_0 is the modulus of elasticity of the pristine material.

As shown in Figure 2, a tri-linear model was adopted to describe the properties of reinforcement bars and steel plates with consideration of the strengthening effect, which can be calculated by Eq.(2).

$$\sigma = \begin{cases} E_s\varepsilon, \ 0 \le \varepsilon \le \varepsilon_y \\ E_s\varepsilon_y, \ \varepsilon_y \le \varepsilon \le k_{s1}\varepsilon_y \\ E_s\left[k_{s4}\varepsilon_y + \dfrac{(1-k_{s4})\times\left(\varepsilon - k_{s2}\varepsilon_y\right)^2}{\varepsilon_y\left(k_{s2}-k_{s1}\right)}\right], \ k_{s1}\varepsilon_y < \varepsilon \le k_{s3}\varepsilon_y \end{cases} \tag{1}$$

where ε_y and σ_y signify the strain and stress at the yield point of the reinforcing steel; E_s represents the elastic modulus of the steel; $k_{s1} = \varepsilon_0 / \varepsilon_y$ is assigned a value of 4.0; $k_{s2} = \varepsilon_b / \varepsilon_y$ is set to 25.0; $k_{s3} = \varepsilon_u / \varepsilon_y$ takes a value of 40.0; $k_{s4} = \sigma_u / \sigma_y$ is established at 1.3. Among these parameters, ε_0 denotes the strain at the onset of hardening of the steel; ε_b corresponds to the peak strain of the reinforcing steel; ε_u is the ultimate strain of the reinforcing steel; σ_u refers to the ultimate stress of the reinforcing steel.

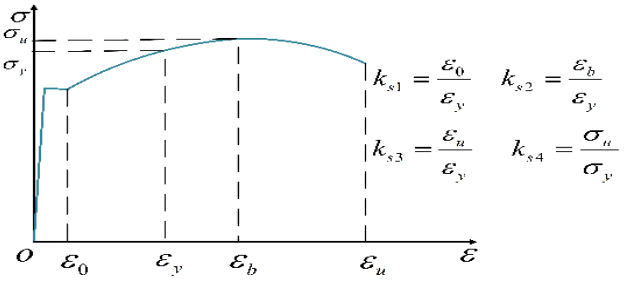

Fig. 2. Stress-Strain Curve of reinforced steels

2.3 Model Construction

The comprehensive model of the tested CSWTG primarily comprises the upper flange concrete slab, corrugated steel web I-beam, longitudinal reinforcements, stirrups, prestressing bundles, encapsulated steel plates, and a concrete bottom plate. The concrete is modeled using C3D8R solid elements with a grid size of 40mm. The reinforcement and prestressing tendons are represented by T3D2 line elements, characterized by an 80mm grid size. The steel plate and corrugated steel plate utilize S4R shell elements, with a 40mm grid size. Notably, the contact interfaces between components do not account for bond-slip phenomena, as the reinforcement, prestressing tendons, and corrugated steel plates are fully embedded within the concrete matrix. The corrugated steel web is anchored to the underside of the upper flange slab. Stress concentration at the loading position is mitigated by employing a rigid loading plate, which is attached to the upper surface of the underlying concrete base plate. The support width is specified at 180mm, and two boundary conditions, namely simply supported and fixed conditions, are implemented. Displacement loading is applied to establish the loading plate and reference point, as illustrated in Figure 3.

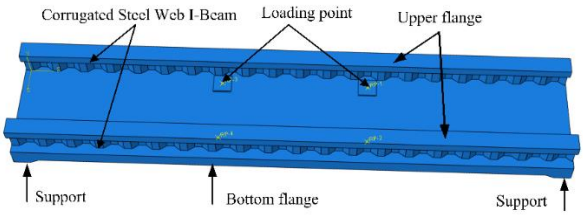

Fig. 3. Load and Boundary Conditions

2.4 Validation of the Model

To assess the mesh sensitivity of the model, mesh sizes of 35mm, 40mm, and 45mm were utilized for both the concrete and steel plates. The corresponding displacement curves are presented in Figure 4. Compared against the experimental data, results from models with mesh sizes of 35mm, 40mm, and 45mm yielded errors of 1.13%, 2.15%, and 0.28%, respectively. Finally, a mesh size of 40mm was chosen for further analysis, considering the balance between accuracy and computational efficiency.

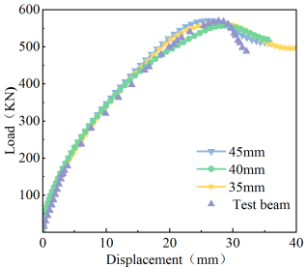

Fig. 4. Comparison Chart of Load-Displacement Curves for Test Beam and Finite Element Simulation

3 Parametric Analysis

As presented in Table 1, a variable parameter analysis was conducted using the calibrated model to examine the influence of various parameters on the torsional capacity, torsional damage, and deformability of CSWTGs. The parameters analyzed included the thickness of the corrugated steel plate h_w, the height-to-span ratio (h/l), the height-to-width ratio of the cross-section (h/w), and boundary conditions.

Table 1. Numerical Model Parameters and Calculation Results

Specimen Number	*h*	*w*	*l*	h_w	*C*	*h/l*	*h/w*	*T*	*θ*
$U_{1\text{-}F}$	510	1200	6000	6	F	1/11.8	1/2.35	288.66	0.0499
$U_{1\text{-}S}$	510	1200	6000	6	S	1/11.8	1/2.35	182.26	0.0228
$U_{2\text{-}F}$	510	1200	6000	10	F	1/11.8	1/2.35	299.28	0.0477
$U_{2\text{-}S}$	510	1200	6000	10	S	1/11.8	1/2.35	203.30	0.0759
$U_{3\text{-}F}$	510	1200	5610	6	F	1/11	1/2.35	297.62	0.0519
$U_{3\text{-}S}$	510	1200	5610	6	S	1/11	1/2.35	169.31	0.0161
$L_{1/11}$	510	1200	5610	6	F	1/11	1/2.35	297.62	0.0519
$L_{1/12}$	510	1200	6120	6	F	1/12	1/2.35	271.97	0.0543
$L_{1/13}$	510	1200	6630	6	F	1/13	1/2.35	258.66	0.0552
$L_{1/14}$	510	1200	7140	6	F	1/14	1/2.35	244.76	0.0721
$L_{1/15}$	510	1200	7650	6	F	1/15	1/2.35	231.02	0.0343
$W_{1/2.16}$	510	1100	6000	6	F	1/11.8	1/2.16	217.47	0.0199
$W_{1/2.35}$	510	1200	6000	6	F	1/11.8	1/2.35	286.66	0.0499
$W_{1/2.50}$	510	1275	6000	6	F	1/11.8	1/2.50	250.39	0.0914
$W_{1/2.75}$	510	1400	6000	6	F	1/11.8	1/2.75	368.66	0.0284
$W_{1/3.00}$	510	1530	6000	6	F	1/11.8	1/3.00	348.79	0.0722
hw_2	510	1200	6000	2	F	1/11.8	1/2.35	201.07	0.0344
hw_4	510	1200	6000	4	F	1/11.8	1/2.35	274.29	0.0592
hw_6	510	1200	6000	6	F	1/11.8	1/2.35	286.66	0.0499
hw_8	510	1200	6000	8	F	1/11.8	1/2.35	291.78	0.0477
hw_{10}	510	1200	6000	10	F	1/11.8	1/2.35	299.28	0.0477

Note: *h* represents the beam height, *w* is the beam width, *l* is the span length, *C* denotes the boundary conditions, *h/l* is the height-to-span ratio, *h/w* is the height-to-width ratio, and *he* refers to the thickness of the corrugated steel, F stands for fixed boundary, S stands for simply supported boundary condition.

3.1 Effect of Corrugated Steel Web Thickness

To investigate the impact of corrugated steel web thickness on the torsional performance of CSWTGs, models with web thicknesses of 2 mm, 4 mm, 6 mm, 8 mm, and 10 mm were constructed and calculated. The corresponding torsional performance curves are depicted in Figure 5. As illustrated, it is evident that the torque progressively increases with the increment of the twist angle and eventually stabilizes. The hw_2 model

exhibits the lowest torsional capacity due to localized buckling damage of the corrugated steel web at the mid-span, whereas the other beams primarily experience typical flexural failure (in Figure 6). When the thickness of corrugated steel web exceeds 4mm, there is a rise in torsional capacity with the increase of web thickness, although the increase is not substantial.

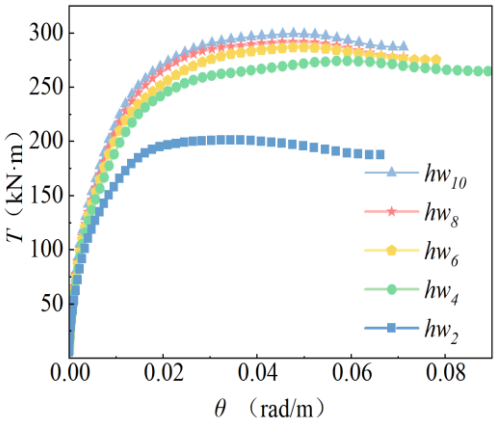

Fig. 5. Torque-angle curves of CSWTGs with different corrugated steel web thickness

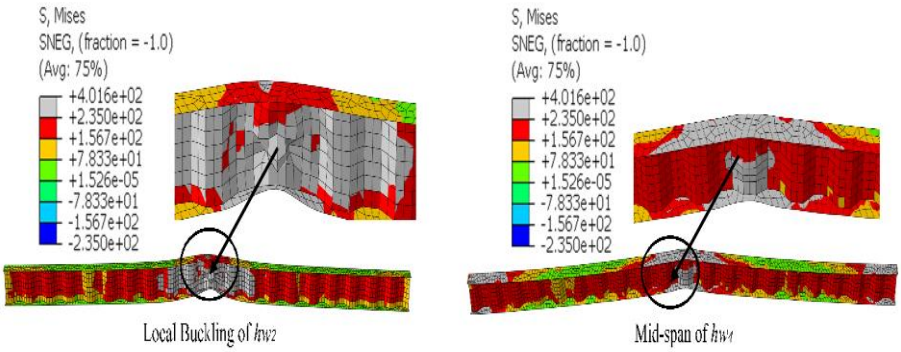

Fig. 6. Failure mode of corrugated steel webs from hw_2 and hw_4 specimens

3.2 Impact of Boundary Conditions

As illustrated in Figure 7, two boundary conditions, fixed condition and simply supported condition, are selected to analyze their impacts on the mechanical properties of CSWTGs by comparing the torque-twist angle curves. It is noted that the fixed condition significantly enhances the ultimate torsional capacity of CSWTGs, with increases of 58.55%, 47.09%, and 75.78% among the three groups, respectively. Besides, torsional stiffness was also strengthened by the fixed boundary condition.

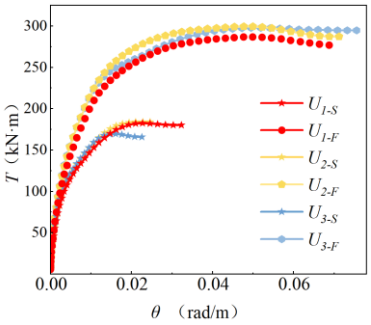

Fig. 7. Torque-angle curves of CSWTGs under different boundary conditions

3.3 Effect of Height-to-Span Ratio

To explore the influence of the height-to-span ratio on the torsional performance of CSWTGs, beams with height-to-span ratios of 1/11, 1/12, 1/13, 1/14, and 1/15 were investigated. The resulting torque-angle curves for each model are illustrated in Figure 8. As shown in the Figure 8, both torsional stiffness and torsional capacity increase with the improvement of height-to-span ratio. The specimens of $L_{1/11}$ possesses the highest torsional capacity of 297.62 KN·m.

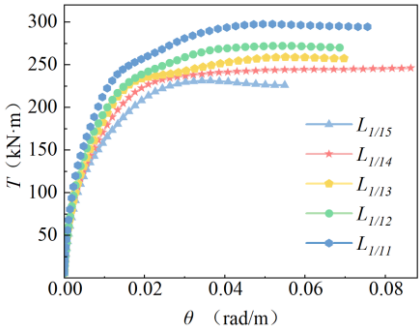

Fig. 8. Results from models with different height-to-span ratios

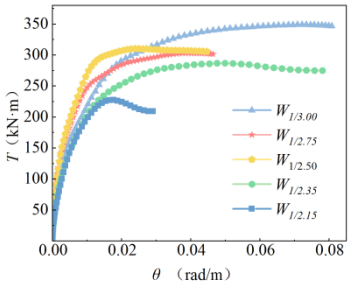

Fig. 9. Results from models with different aspect ratios

3.4 Effect of Aspect Ratios

To investigate the impact of aspect ratio on the torsional performance of CCSWs beams, specimens with aspect ratios of 1/2.16, 1/2.35, 1/2.50, 1/2.75, and 1/3.00 were selected. The aspect ratio variation was determined by adjusting beam width. The corresponding curves for each CSWTG model are illustrated in Figure 9. As depicted, the ultimate torsional capacity increases as the aspect ratio decreases. The $W_{2.15}$ model shows the least torsional capacity and experiences a significant drop after its peak point. However, the torsional stiffness of the $W_{2.50}$ model is the highest. The other models exhibited relatively lower torsional stiffness which may be influenced by the shear effects in models with high aspect ratios.

4 Conclusion

(1) When $h_w < 2$ mm, the ultimate torsional capacity of the CSWTGs sharply decreases because of the premature failure caused by the overall buckling of corrugated steel web; On the other hand, a typical flexural failure mode occurred in the CSWTGs with corrugated steel web thickness higher than 4mm, leading to a 30%~50% improvement of ultimate torsional capacity. Meanwhile, the torsional capacity increases with the thickness of the corrugated steel web, although the increment is not substantial.

(2) Compared to simply supported condition, fixed condition can significantly enhance the torsional capacity (increased by 75,78% averagely) and torsional stiffness of CSWTGs. Besides, torsional capacity of CSWTGs increases with the increase in height-to-span ratio and the decrease in aspect ratio.

Reference

1. Chen S, Diao B, Guo Q, et al. Experiments and calculation of U-shaped thin-walled RC members under pure torsion[J]. ENGINEERING STRUCTURES. 2016, 106: 1-14.
2. Chen Shenggang, Li Chaolai, Diao Bo, et al. Finite element analysis of U-shaped RC beams under pure torsion[J]. Journal of Building Structures. 2020, 41(S1): 230-237.
3. Shenggang C, Chaolai L, Quanquan G, et al. Computational analysis of shear deformation effects on open thin-walled beams[J]. Structures. 2022, 36: 678-690.
4. Xu J, Diao B, Guo Q, et al. Interaction of bending, shear and torsion in U-shaped thin-walled RC girders[J]. ENGINEERING STRUCTURES. 2019, 179: 655-669.
5. Xu J, Chen S, Guo Q, et al. Experimental and Analytical Studies of U-Shaped Thin-Walled RC Beams Under Combined Actions of Torsion, Flexure and Shear[J]. INTERNATIONAL JOURNAL OF CONCRETE STRUCTURES AND MATERIALS. 2018, 12(1): 272-278.
6. Qian Jianqi, Hailong Z, Yang Ming, et al. Restudy of calculation method of cross-section bending capacity for preflex composite beams [J]. Journal of Harbin Institute of Technology. 2022, 54(03): 65-73.
7. Zhuo-Yi C, Chuan-Xi L, Qiao H, et al. EXPERIMENTAL STUDY ON TORSIONAL PROPERTY OF COMPOSITE TROUGH GIRDER WITH CORRUGATED STEEL WEBS[J]. Engineering Mechanics. 2017, 34(03): 108-114.

8. Yang M, Tian L, Yuan Y, et al. The study on composite trough beam with corrugated steel web wrapped with steel plate: Experiment and bending properties[J]. JOURNAL OF CONSTRUCTIONAL STEEL RESEARCH. 2021, 185: 106853.